Munz *et al. Microplastics and Nanoplastics* (2024) 4:2
https://doi.org/10.1186/s43591-023-00077-z

Microplastics and Nanoplastics

RESEARCH

Open Access

Transport and retention of micro-polystyrene in coarse riverbed sediments: effects of flow velocity, particle and sediment sizes

Matthias Munz[1], Constantin Loui[1*], Denise Postler[1], Marco Pittroff[1,2] and Sascha E. Oswald[1]

Abstract

Riverbed sediments have recently been found to be an important reservoir for microplastics. But the hydrogeological factors that control the abundance of microplastics are complex and conceptual frameworks priorising the parameters affecting their transport and retention during deep riverbed filtration are still missing. In this study a series of saturated column experiments was conducted to investigate the vertical distribution patterns of secondary polystyrene fragments (100–2000 µm) in dependence on their particle size, grain size of the sediment, seepage velocity and duration of infiltration flow. The columns with a length of 50 cm were operated with flow velocities between 1.8 m d^{-1} and 27 m d^{-1}. Invasive samples obtained after the experiments were density separated and then depth profiles of microplastic concentrations were retrieved using fluorescence imaging analysis. Most polystyrene particles were retained in the upper 20 cm and 15 cm of the medium gravel and coarse sand sediments, respectively. Through the high particle retention riverbed sediments can act as a temporary sink or long term retention site for the transport of microplastic particles (MPPs) from streams to oceans. A small fraction of particles ranging from 100 to 500 µm in size was observed down to infiltration depths of 50 cm suggesting that MPPs at the pore scale have the potential to be advectively transferred via hyporheic exchange or induced bank filtration into coarse riverbed sediments and alluvial aquifers. MPP abundance over column depth follows an exponential relationship with a filter coefficient that was found to depend significantly on the flow rate, MPP and sediment grain size, as indicated by multiple linear regression ($R^2 = 0.92$). The experimentally derived empirical relation allows to estimate particle abundances of initially negatively buoyant MPP in riverbed sediments by surface water infiltration.

Keywords Microplastic, Column experiment, Saturated sediments, Riverbed, Fluorescence microscopy

Introduction

Microplastics particles (MPPs) are ubiquitous in freshwater ecosystems such as rivers, riverbed sediments, possibly even in groundwaters [17, 20], serve as mobile carriers of pollutants [1, 36] and potentially threaten soil microbial communities, enzymatic activities, and human health [32, 35, 36].

Rivers play an important role in the transport of plastic into lakes, seas, and oceans [10]. Microplastics concentrations in rivers vary over a wide range, and may exceed several thousands of particles per cubic meter of river

*Correspondence:
Constantin Loui
constantin.loui@uni-potsdam.de
[1] Institute of Environmental Science and Geography, University of Potsdam, Karl-Liebknecht-Str. 24-25, 14476 Potsdam, Germany
[2] BAW, Federal Waterways Engineering and Research Institute, Kußmaulstr. 17, 76187 Karlsruhe, Germany

water in urbanized areas [17, 38, 39]. The particle density, shape, and size as well as as physicochemical or biotic interactions determine whether MPP can be buoyant, neutral or sink in surface waters [19, 37, 46]. For polystyrene particles (100–1000 µm), for instance, the modelled mean residence time in the epilimnion (2–18 m) of a stratified lake was estimated to be less than 1 day. In contrast, for the smallest microplastic particles (<= 30 µm) the mean residence times were orders of magnitudes higher [12]. As a result, especially the smallest fraction of MPP tend to float in the water column and may never reach bed sediments. In stream ecosystems hyporheic exchange is considered as an important mechanism for the exchange of water and energy between water column and bed sediments [27] and for the delivery of microplastic particles to the streambed [11].

A certain number of MPP sink onto, infiltrate and accumulate in riverbed sediments [2, 29]. Recent studies examined the spatial and temporal distribution of microplastics in top riverine sediments worldwide, often with highest abundance of PE, PP, and PS [18]. In sediment samples from the *Thames River* (Canada), Corcoran et al. [7] found the highest number of MPPs in samples with the finest grain size and with the highest portion of organic debris. Apart from that, MPPs can be remobilized into the surface water, transported and reemerged into the water column via hyporheic flow paths [11] or further relocated into the aquifer. In bank filtrate of an sandy to gravelly, alluvial aquifer (adjacent the *Lower Havel River*, North-East Germany) and in raw drinking waters exclusively from groundwater (Oldenburg, North-West Germany) only low concentrations of 4 MPP m^{-3} (100–700 µm) [25] and of 0.7 MPP m^{-3} (50–150 µm in size) [24] were detected, respectively. But studies analysing even smaller particles found much higher concentrations of 197 MPP m^{-3} (MPPs > 5 µm, South-West Germany) [30] and of 3.6 * 10^6 MPP m^{-3} (MPPs > 1 µm, Czech Republic) [31] in raw drinking water. Detected particles were mostly identified as PE, PA, PET, PVC, PS or epoxy resin.

Microplastic abundances in riverbed sediments are difficult to detect and so far only a few studies are available. Microplastic abundances can exhibit a clear decreasing trend with increasing depth. Fraser et al. [14] highlighted that the mean abundance of microplastic (50–5000 µm) in *Tonglu* and *Fuyang* riverbed sediments (China), that were collected with a gravity corer, significantly decreased from 290 MPP kg^{-1} (surface sediments), via 130 MPP kg^{-1} (5–10 cm) to 60 MPP kg^{-1} (10–15 cm). PE, PS, and PET fragments were the dominant polymer types present in sediment samples and accounted for 86–98% of the total abundance. And 63% of MPPs at 10–15 cm were larger than 100 µm.

Frei et al. [15] found highest MPP accumulation for particle sizes from 20 to 500 µm in the upper 10 cm (exceeding 50,000 MPP kg^{-1}) of five freeze cores extracted from the *Roter Main River* sediments (Germany), consisting of high fractions of sand, medium to fine gravels and cobbles. MPP concentrations generally decreased with increasing depth (60 cm) except for the 10–20 cm segment where the lowest particle abundance (≈10,000 MPP kg^{-1}) was detected. Large PS particles (500–5000 µm) were found down to a depth of 60 cm below the streambed surface.

However, also other types of microplastic distribution in riverbeds can occur, for example, microplastic concentrations were found to increase from shallow to deep layers in *Qinhuai River* sediments (China) mainly composed by silt [28]. The mean MPP concentration across 15 sites gradually increased with increasing depth from 20 MPP kg^{-1} (0–10 cm) to 47 MPP kg^{-1} (41–50 cm) when analysing 10 cm thick segments. The average number of MPP < 2 mm in each layer across 15 sites increased gradually with depth, whereas the number of largest microplastics (> = 2 mm) decreased with the increasing depth [28]. Thus, the riverbed could represent an important reservoir for microplastics and may act as a long-term pollutant sink, provided that the previously deposited microplastics are not fully remobilised or substantially carried into aquifers.

Soil column or lysimeter experiments can be very helpful in order to better understand distribution patterns of MPPs as observed in the environment and to obtain a better grasp on their transport processes in unsaturated and saturated sediments. Column experiments are commonly conducted with well-characterized granular media (e.g., glass beads, gravel or sand) to explore the physical and chemical influences on the transport and retention of microplastic particles in porous media via monitoring changes in the column effluent microplastic concentration as a function of time or detecting microplastic retention profiles.

For saturated conditions as in riverbed sediments, studies so far focused on transport of micron sized plastic PS spheres (< 10 µm), thus a primary MPP. For them, particle mobility decreased and deposition increased for increasing ionic strength, lower flow rates, and larger ratio of the colloid to the median grain diameter [3, 4, 9]. Furthermore, the aggregation kinetics of MPP is an important factor in controlling their environmental fate and transport, whereby the aggregation of PS particles among themselves in freshwater environments (i.e. lakes and rivers) is unlikely [8, 21]. Dong et al. [9] found that 2 µm sized PS were not retained in sand columns operated with deionized water. The ionic strength and diameter of the collector

and MPP were the dominant factors affecting the retention of plastic colloids [22], however, just for glass beads as porous medium.

Most of the current experimental works use small size spherical particles, while MPPs in the environment have various shapes and sizes that may affect their transport. Recently some studies also focused their observations on larger microplastics, such as fragments [43, 45]. Microplastic fragments could possibly even be detected within undisturbed sediment cores by tomographic methods [41, 42]. Concordantly, particles > 100 µm were found to be mobile in unsaturated laboratory experiments with glass beads; the infiltration depth increased with smaller particle-to-grain size ratios [45]. According to these authors, 100 µm sized MPPs can penetrate to an average depth of 0.13 m in coarse sand and fine gravel, whereas 1000 µm sized MPPs are only detectable to 0.01 m in coarse sand and 0.05 m in fine gravel.

Despite an increasing number of studies the source, transport and fate of MPPs in streambed sediments remain unclear [44]. To gain a better understanding of the transport and retention of irregularly shaped microplastics in water saturated sediments we investigated and statistically analysed the abundance, distribution and retention of secondary polystyrene particles (100–2000 µm) in column experiments, with regard to dependence on flow rate, duration of infiltration event, particle size and sediment grain size.

Materials and methods

Sediment and microplastic particles

As an analogue to coarse-grained river sediments, medium gravel ($d_{10}/d_{50}/d_{90}$: 5.60/6.60/7.80 mm) and coarse sand ($d_{10}/d_{50}/d_{90}$: 1.13/1.51/1.90 mm) was used in the column experiments as porous media (Fig. 1a). Before use, the rounded, pH neutral, organic free sediments (provided by supplier Steinlando GmbH & Co. KG according to DIN 53200) were rinsed with tap water in stainless steel sieves with a mesh size of 2 mm (medium gravel) or 1 mm (coarse sand) until the water was clear and then they were dried at 100 °C for 24 h.

Fragments of solid, fluorescent polystyrene (PS), that offer a simple and reliable detection with fluorescence microscopy [23], were produced by cryomilling (Retsch UZM 100) red fluorescent polystyrene ($\rho \approx 1.06\,g\,cm^{-3}$) granulate (Magic Pyramid) and fractionated into the size classes 100–250 µm, 250–500 µm, 500–1000 µm and 1000–2000 µm using stainless steel sieves (for particle identification and size quantification see section 2.4). The resulting fragments were completely stained with the fluorescent dye. In order to remove any grinding dust adhering to the particles, the PS were rinsed with deionized water and 30% ethanol solution, dried at 60 °C and stored in the dark in amber glass bottles until use. The excitation and emission wavelength of these particles were at 550 ± 25 nm and 605 ± 70 nm, respectively.

For each column experiment 5 mg of PS per size class was weighed out using a precision balance (Mettler Toledo

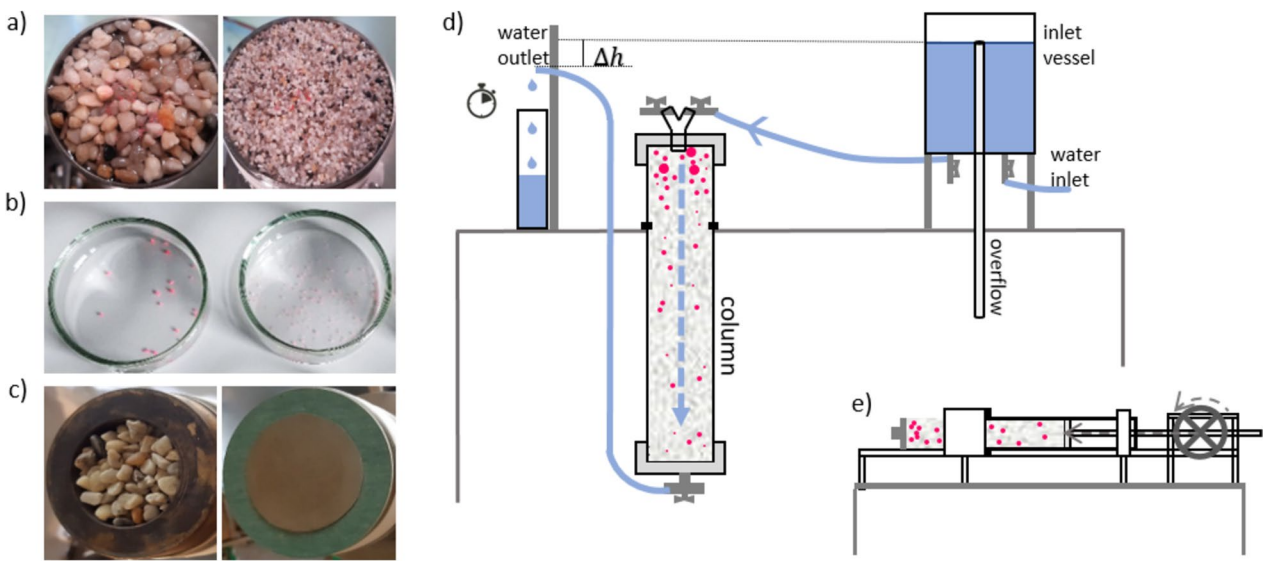

Fig. 1 **a** Top view of columns (Ø = 8 cm) filled with medium gravel, d_{50} = 6.60 mm (left) and coarse sand, d_{50} = 1.51 mm (right); **b** Fragments of fluorescent polystyrene particles within size class 500–1000 µm (left) and 250–500 µm (right); **c** Top view of columns covered with brass spacer ring filled with gravel (left) as well as sealing ring and 10 µm stainless steel mesh (right); **d** Sketch of the column setup (not to scale; column Ø = 8 cm and L = 50 cm); and **e** Sketch of the self-made sediment extraction pushing device

NewClassic ML, linearity = 0.0002 g) and transferred to glass petri dishes (Fig. 1b). The average number of MPPs added to the columns depended on the size class and ranged from 1365 ± 314, 541 ± 48, 67 ± 5 and 9 ± 1 for the size classes 100–250 µm, 250–500 µm, 500–1000 µm and 1000–2000 µm, respectively (Table S1 in Supporting Information).

Column preparation and operation

Stainless steel columns with a length of 50 cm and an inner diameter of 8 cm (volume ≈ 2.5 dm^3) were used for the laboratory experiments. The rinsed sediment was gradually filled into the column with a metal funnel while lightly tapping the column with a rubber mallet and saturating from below with tap water. Through the tapping and saturation, the sediment was compacted and air inclusions could escape.

A sealing ring (aramid fibers/NBR binder), a 10 µm stainless steel mesh and a 2 cm thick brass spacer ring that was filled with medium gravel were put on top of the packed column (Fig. 1c) and covered with the sealing cap with a 3/8″ two-way ball valve for PTFE hose connections. The lower sealing cap was connected with a PTFE hose with an inner diameter of 11 mm to the inlet vessel. The column experiments were operated using tap water (chemical parameters are listed in Table S2 in the supporting information). The total porosity of the sediment was calculated as the ratio of pore to column volume. The pore volume was estimated via the weight difference between the dry and the water saturated column divided by the density of water.

To mimic surface water infiltration into riverbed sediments the columns were operated in downward flow direction driven by a free gradient instead of the much more common used upward flow direction driven by a peristaltic pump [8, 43]. This ensures that the direction of gravity forces is in the direction of flow. Before starting the column experiments each column was flushed with at least three pore volumes of water (≈3000 ml in total) and the flow rate was adjusted by changing the pressure difference between in- and outlet (Δh, Fig. 1d). An indirect determination of the column flow rate (Q [ml min^{-1}]) was performed via repeated measurements of time needed to collect 100 ml of effluent.

Once the flow rate had reached equilibrium, the flow was interrupted, the column was opened and drained by only a few millilitres, and the PS particles were added to the sediment surface. The Petri dishes used as well as tweezers and spatulas were rinsed with deionized water over the sediment surface to release any remaining MPP while at the same time refilling the column by the previously drained water volume. The column was closed again and the experiment was started with the afore established flow rate. Despite the risk of getting hydraulic artefacts in the column, this experimental approach was preferred over adding particles to the water reservoir and maintaining the predetermined flow rate, as this alternative would lead to experimental difficulties such as keeping the MPPs in dispersion, fixing a constant MPP concentration in the reservoir or avoiding possible MPP adhesion in the pipes.

A series of 11 column tests was carried out including

- five different flow rates (Q) ranging between 4 ml min^{-1} and 40 ml min^{-1} in columns filled with medium gravel (mGr). These columns were named according to their flow rate and the used sediment (e.g. Q4_mGr or Q13_mGr),
- two different Q of 2 ml min^{-1} and 4 ml min^{-1} in columns filled with coarse sand (cSa) (e.g. Q4_cSa), and
- different durations. If not mentioned otherwise experiments were conducted for a duration until about eight pore volumes (PV) passed the columns. If the duration was adapted to shorter times, the column names were extended by the duration of the experiment (e.g. Q10_mGr_4PV or Q10_mGr_2PV).

The flow rate was measured regularly approximately every 15 minutes. Despite all efforts and adjustments in the experimental setup the flow rates slightly varied over time for each experiment (Table 1). At the end of each experiment the columns were drained while maintaining the afore established outflow rate (though for the first columns Q38_mGr and Q20_mGr in a less stringent way than for the others).

The predefined exchange conditions agree well with water fluxes observed in surface water groundwater systems, ranging from tens of meters per day of hyporheic exchange flow in gravelly mountain streams (e.g. [48]), via a few meters per day in flood affected bank filtration systems in gravelly aquifers (e.g. [47]), to about 1 meter per day in bank filtration systems in sandy to gravelly aquifers during base flow conditions (e.g. [26]).

Sediment sampling and PS extraction

After the column transport experiments the sediment was sampled as 2.5 cm segments for the topmost 5 cm of the column and in intervals of 5 cm for the rest of the column from 5 to 50 cm. The sediment was carefully removed with a stainless-steel spoon down to 15 cm for all columns filled with medium gravel and down to 20 cm for all columns filled with coarse sand. To sample the sediment below that depth it was pushed out of the column using an individually manufactured sediment extraction pushing device (Fig. 1e). All sediment samples were transferred to 250 ml (2.5 cm intervals) or 500 ml (5 cm

Table 1 Overview of experimental conditions. Q_{mean} is the average flow rate, std. is the standard deviation of Q and v_a is the average seepage velocity of each column ($v_a = \frac{Q_{mean}}{\theta \cdot A_{column}}$). The volume of the columns is ≈1000 ml

experiment	porosity θ [–]	Q_{mean} [ml min^{-1}]	std(Q) [ml min^{-1}]	v_a [m d^{-1}]	std (v_a) [m d^{-1}]
Q38_mGr	0.38*	37.7	0.3	27.7	0.2
Q20_mGr	0.38*	19.9	0.5	14.6	0.4
Q13_mGr	0.38*	13.2	0.7	9.7	0.5
Q4_mGr	0.38	3.9	2.0	2.9	1.5
Q10_mGr_4PV	0.37	10.3	1.2	7.8	0.9
Q10_mGr_2PV	0.39	9.9	1.7	7.1	1.2
Q4_cSa	0.36	4.5	1.4	3.5	1.1
Q2_cSa	0.37	2.4	1.1	1.8	0.8
Q6_cSa_2PV	0.37	6.4	3.0	4.8	2.1
Q11_cSa_4PV	0.38	11.3	2.7	8.3	1.9

* estimated value (average porosity of all gravel filled columns)

intervals) wide neck Erlenmeyer flasks, dried at 60 °C for at least 48 h and weighted (Table S3 in Supporting Information).

In order to separate microplastic particles from the denser matrix components we used a sodium chloride solution (NaCl) with a density of at least 1.2 g cm^{-3}. The Erlenmeyer flasks were approximately half-filled with the density solution, stirred for 2 min with a stainless-steel spatula (I) and treated for 2 min in an ultrasonic bath (II) to destroy soil agglomerates (steps I and II were repeated once more). Afterwards, the Erlenmeyer flasks were filled with the density solution and left for 24 h in the dark. Subsequently, all floating compounds were decanted or captured by direct vacuum filtration. The fluorescent particles were clearly visible under normal laboratory conditions. This also applies for the smallest fraction of 100–250 µm. Visual inspection of the remaining sediment after density separation revealed no visible evidence of fluorescent MPPs, thus confirming that the overwhelming majority of particles were successfully separated.

During the decantation, the Erlenmeyer flask was rotated slowly so that particles adhering to the inner wall of the flask were flushed out and the eluate was poured through a vacuum filtration unit on glass fibre (GF) filters (ROTILABO® Typ CR263, Ø: 47 mm, mesh size: 0.7 µm) with a hand vacuum pump. The GF filters were regularly replaced in dependence of the captured number of PS and other particles to avoid particle overlays and touches while maintaining a manageable number of filters. In average 5.2 filters were used per sediment sample. In order to reduce the number of filters, this method used for Q38_mGr and Q20_mGr was replaced by vacuum filtration.

For direct vacuum filtration (PC 3001 VARIO select) the flotate in the Erlenmeyer flask was sucked off with a silicone hose up to the lower end of the flask neck and refilled with NaCl solution. This process was repeated three times. After the third filling, the separation solution was sucked off up to approx. 1 cm above the sediment. All floating compounds were captured through a filtration funnel on a 10 µm stainless steel mesh (Sartorius) and transferred to a GF filter (ROTILABO® Typ CR263). In average 2.4 filters were used per sediment sample. All GF filters were transferred to glass petri dishes, covered with aluminium foil and placed in the drying oven at 60 °C. Average particle count for the filters of the first sediment layer (0–2.5 cm, highest MPP occurrence) was 286 ± 110.

To avoid sample contamination all materials were rinsed intensively with deionized water and ethanol solution and placed in the ultrasonic device. Two blank filters were processed within each column test ($n = 20$). For that 250 g of the sediment used for the column filling was transferred to a 250 ml Erlenmeyer flask and processed in the same way as the column sediment samples.

PS detection and characterisation

To detect the fluorescent PS particles all sample filters were scanned using the fluorescence imaging system ChemiDoc (Bio-Rad Laboratories, Inc). The MPPs on the filters were excited for 0.003 s using green coaxial illumination (*green epi illumination*) and one image per filter was recorded in the range of 602 ± 50 nm using an integrated CCD camera allowing low-noise recording with a pixel resolution of 32.7 µm.

For the characterization of particle dimensions, each recorded image was evaluated using ImageJ [33, 40]. Image analyses included Non-local Means Denoising [5], Thresholding, Watershed analyses and Particle analyses (Rasband, 1997–2018) in order to calculate the properties of each particle region, such as area, circumference, minimum Feret diameter and circularity. If the number of neighbouring pixels with a relevant fluorescence signal

was larger than two they were classified as one microplastic particle. Consequently, the limit of detection was roughly 100 µm. Then the minimum Feret diameter was evaluated, for which ImageJ selects the minimum distance between two parallel tangents of the particle positioned in any arbitrary angle around the x- or y-axis (minimum calliper around the particle). The minimum Feret diameter was chosen because it is expected to be the minimum size that could just allow MPPs to penetrate through the sediment pore throats. Furthermore, the reliability of the analytical MPP detection and characterisation was verified with a recovery test of 80 (20 per size class) randomly selected particles. The dimensions of those particles were additionally measured using fluorescence phase contrast microscope (KEYENCE Biozero BZ) to identify the linearity and offset between both methods (results are presented in section 3.1.).

Based on the minimum Feret diameter the relative MPP abundance (C_L/C_{Tot}) per size class (L) and depth segment (z) was calculated as:

$$\frac{C_L}{C_{Tot}}(z) = \frac{n_{z,L}}{m_z} / \sum_{z=2.5}^{50} \frac{n_{z,L}}{m_z} \tag{1}$$

where C_L is the MPP concentration [MPP kg^{-1}], C_{Tot} is the input particle concentration in the column [MPP kg^{-1}], $n_{z,L}$ is the number of particles of a certain segment and size class and m_z is the dry mass of the sediment segment taken (Table S3 in Supporting Information).

Microplastic particle retention

The relative particle abundance versus depth after several PV were flushed through (retention profile) can be described by first-order reaction kinetics [16]:

$$\frac{C_L}{C_{Tot}}(z) = e^{-\lambda_L \cdot z} \tag{2}$$

where λ_L [cm^{-1}] is the filter coefficient of a clean filter medium in respect to a certain particle size class (L). According to that, particle abundance in a porous medium decreases exponentially with depth (z). For the shallowest sampling interval (0–2.5 cm) z was assigned to be 0 because a large amount of MPPs were present on top of sediment whereas for all other sampling depth intervals z was ascribed to the midpoint of the segment. As particle retention is strongly dependent on particle size eq. 2 strictly applies only for a suspension uniform in size, i.e. monodisperse (particles of a certain size class). The filter coefficient was evaluated by fitting eq. 2 to the measured retention profiles by minimizing the root mean square error ($C_L/C_{Tot} > 0.023$, below this threshold, the particle abundance does not necessarily decrease exponentially with increasing depth, but rather remains constant for low values with increasing depth, see section 3.2).

To relate the λ_L to our set of experimental conditions (predictors, such as flow velocity, sediment grain and MPP size) we applied a generalized multiple linear regression model (GLM) (implemented in the R-package 'stats') [6, 34]:

$$\lambda_L{}^* = \beta_0 + \beta_1 \times \frac{minFeret_L}{minFeret_{L,mean}} + \beta_2 \times \frac{v_a}{v_{a,mean}} + \beta_3 \times \frac{d_{50}}{d_{50,mean}} + \varepsilon \tag{3}$$

where $minFeret_L$ is the average minimum Feret diameter of all particles within a size class, v_a is the average seepage velocity, and d_{50} is the mean porous media grain size. In order to obtain a dimensionless form of the predictors, they were divided by their respective mean values (*mean*). The coefficients β_i [i = 0...3], representing the individual effect of each predictor variable on λ_L, are adjusted to minimize the error term (ε) based on the sum of squared errors. For the GLM the response variable λ_L is transformed with a link function ($\lambda_L{}^*$) to accommodate for non-normal conditional distributions [13]. An appropriate link function enhances the prerequisites (normal distribution of error terms, homoscedasticity, and absence of multicollinearity) of multiple linear regression models. The obtained regression coefficients allow the interpretation of the predictors' influence on the filter coefficient.

Results and discussions

Microplastic particle detection and laboratory blanks

The recovery test of 80 randomly selected particles (20 per size class) proved the high accuracy of the analytical particle identification and quantification procedure. All fluorescent PS on the filters were correctly assigned as particles (recovery = 100%) and the false discovery rate was only 1.3% (precision = 98.7%), i.e. just on one filter a pixel group wrongly indicated the presence of a MPP 130 µm in size (constituting a single false positive). The false positive identification of a filter area seemed a result of fluorescence scattering from larger MPPs when not fully removed by the application of Non-Local Means Denoising and Thresholding. This implies that such false positive detects will not occur if there are no real MPPs on a filter. Furthermore, all identified particles were detected with an accurate size (no systematic over- or underestimation). The relation between minimum

Feret Diameter derived with the automated particle identification and quantification procedure and individual size estimates with the fluorescence phase contrast microscope was found to be linear with a slope of 0.95 ($R^2 = 0.96$) (Fig. S4 in Supporting Information). Recovery rates were determined for five of the column experiments carried out (Tab. S1 in Supporting Information). Average MPP recovery rate was 84%.

In total 12 fluorescent particles with an average size of 260 µm were found on 8 out of the 20 blank controls. A maximum of two particles were found in the size classes between 100 and 250 µm and 250–500 µm on any blank control. These particles could have adhered to any of the experimental columns (e.g. valves) or materials used for MPP extraction (e.g., pipes or sealings) and thus been transferred to the blanks from previously processed columns. This is more fluorescent particles on the blanks than desirable, but has to be seen in relation to the high number of detected particles on each filter. As this constitutes only 0.11% of the average number of MPPs on a filter, it follows that a contamination of the analysed samples by fluorescent PS is rather negligible.

Microplastic particle retention

Gravel packed columns

The relative particle abundances found in the first 2.5 cm strongly varied with the flow rate. Relative abundances of microplastic particles between 100 and 250 µm ranged between 0.47 and 0.86 for the flow rates of 38 ml min^{-1} and 4 ml min^{-1}, respectively. Generally, the abundance of larger particles in 2.5 cm and 5 cm is higher compared to smaller particles whereas this relation inverted with increasing depth (Fig. 2). All MPPs larger than 1000 µm were retained in the uppermost 5 cm (Table 2). Particles in between 500 and 1000 µm penetrated to an average depth of 20 cm whereas smaller particles were partly found over the entire length of the experimental columns (Table 2). A minor fraction of particles < 500 µm were relocated to depths below 20 cm of the gravel packed columns for flow rates equal and higher than 13 ml min^{-1} (Fig. 2a&b, Fig. 3c). For those conditions the relative MPP abundance from 20–50 cm remained quite constant with average values of 0.023 (73 MPP kg^{-1}) and 0.012 (26 MPP kg^{-1}) for size classes of 100–250 µm and 250–500 µm, respectively (Fig. 2& 3).

The maximum ratio of MPP size to sediment grain size required to allow for MPP infiltration below 20 cm in our experimental columns was about 0.08, which is somewhat smaller than the relation of 0.11 proposed by Waldschläger and Schüttrumpf [45] inferred from unsaturated experiments with spherical glass beads; i.e. the maximum MPP size that was found to infiltrate into sediments in our saturated experimental columns was just slightly lower (by a factor of 0.77) compared to Waldschläger and Schüttrumpf [45]. Even if saturated and unsaturated

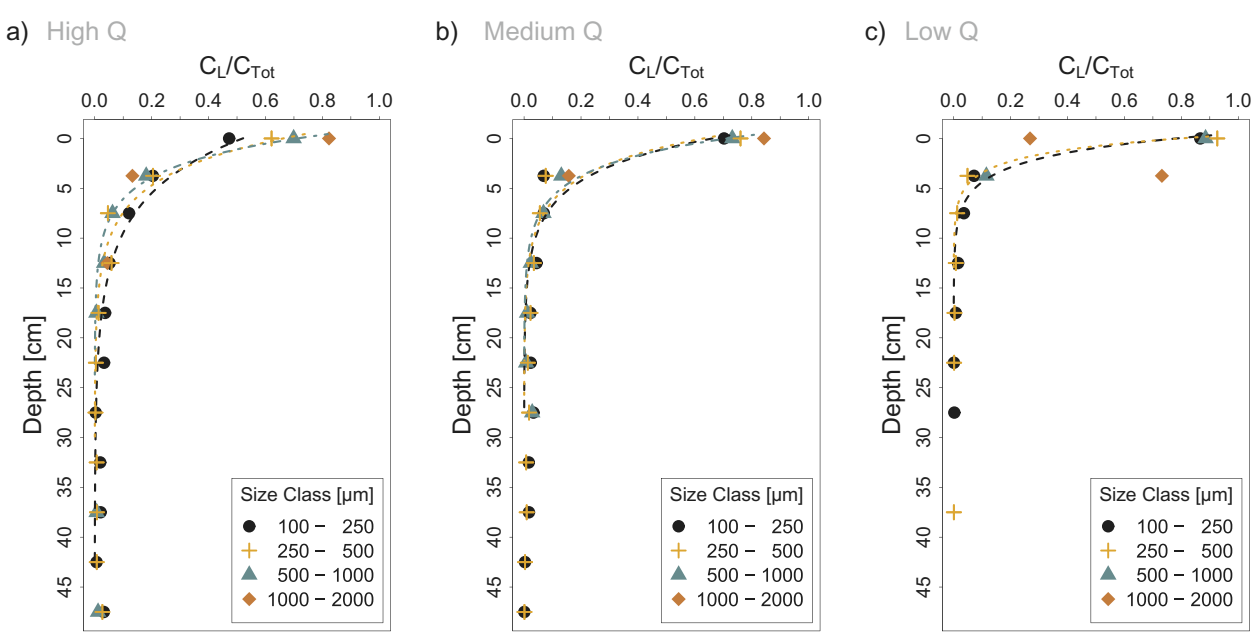

Fig. 2 PS retention profiles for the gravel packed columns operated with flow rates (Q) of about 38 ml min^{-1} (**a**, Q38_mGr), 20 ml min^{-1} (**b**, Q20_mGr) and 4 ml min^{-1} (**c**, Q4_mGr)

Table 2 Maximum penetration depth (depth in which particles are not present for the first time when screening downwards) for each experiment depending on particle size class

Column name	Maximum particle penetration depths [cm]			
	100–250 µm	250–500 µm	500–1000 µm	1000–2000 µm
Q38_mGr	> 50	> 50	25	5
Q20_mGr	> 50	> 50	30	5
Q13_mGr	> 50	> 50	20	5
Q4_mGr	30	25	5	5
Q10_mGr_4PV	35	25	10	2.5
Q10_mGr_2PV	40	30	10	2.5
Q4_cSa	15	20	2.5	2.5
Q2_cSa	10	15	2.5	2.5
Q6_cSa_2PV	25	5	2.5	2.5
Q11_cSa_4PV	25	10	2.5	2.5

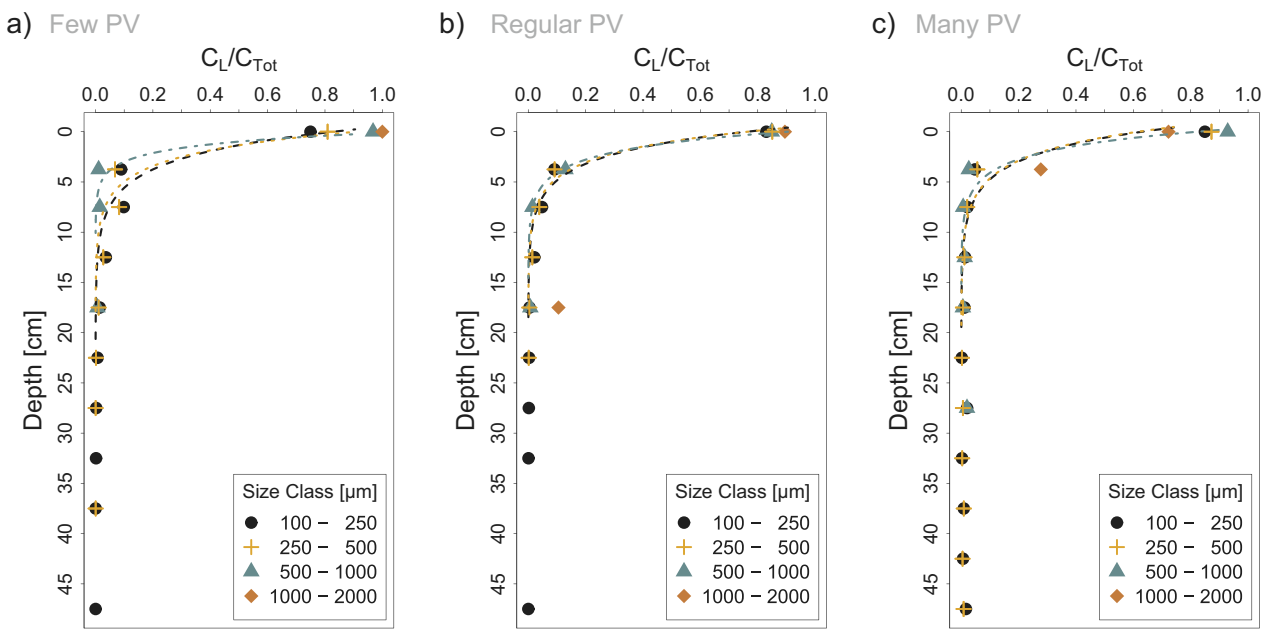

Fig. 3 PS retention profiles for the gravel packed columns operated with comparable flow rates of about 10 ml min^{-1} (**a** & **b**) and 13 ml min^{-1} (**c**), but with different duration of infiltration that is pore volumes (PV) passed through. Applied flow volumes were about 2 PV (**a**, Q10_mGr_2PV), 4 PV (**b**, Q10_mGr_4PV) and 8 PV (**c**, Q13_mGr)

flow conditions could not be exactly compared to each other such differences might result from deviations in water fluxes through the experimental columns (0.7 ml min^{-1} cm^{-2} in our study vs. 15.6 ml min^{-1} cm^{-2} in Waldschläger and Schüttrumpf [45]).

Sand packed columns

Particles above 500 µm were retained in the uppermost 2.5 cm of the sandy column fillings (Table 2, Fig. S5 in Supporting Information). Smaller particles infiltrated to an average depth of 15 cm. Average particle abundances of size classes of 100–250 µm and 250–500 µm at a depth of 15 cm were below 4.5×10^{-3} (8 MPP kg^{-1}) and 2.1×10^{-3} (4 MPP kg^{-1}), respectively. The maximum particle penetration depths in the sand columns were found to be higher than those of Tumwet et al. [43] who found maximum penetration depth of 2.5 cm for PVC of 125–200 µm, comparable sediment sizes (1.6–2.0 mm) and applied water fluxes (0.7 ml min^{-1} cm^{-2}, ultrapure water). Under these experimental conditions, spherical LDPE particles did not even migrate from its initial position.

Variation in duration of infiltration flow

We observed comparable spatial patterns of particle abundances for the gravel packed columns when operated with different pore volumes, that is different duration of the infiltration flow. Again, the particle abundance of all size classes strongly decreased with depth. The highest number of particles of all size classes were found in the first 2.5 cm of the sediment (Fig. 3). Slight differences were observed in the maximum particle penetration depths (Table 2), which can also be caused by not exactly identical exchange flows besides the variations in the applied flow volume. Thus, the retention of MPPs was found not to be dependent on extending the flow duration beyond 2 PV. Due to the slightly varying flow throughout the column experiments the effect of infiltration duration on the particle retention profiles could not be further quantified. However, for the studied range of variation in flow durations the experimental results so far indicate that extending the duration had a negligible effect on the retention profiles (Fig. 3), compared to the variation in column filling material and flow velocity. The reason seems to be that a steady particle retention profile quickly established within the very first exchanged pore volumes, and not much further transport of the microplastic particles occurred when already retained in the column, at least for the stable hydrochemical and hydrodynamic conditions of our experiment.

Influence of experimental parameters on the filter coefficient

The filter coefficient (λ_L) was optimised for each individual experiment in order to achieve the best fit between theoretical (eq. 2) and measured particle retention profiles. The optimized filter coefficient, describing the local decrease in particle abundance with depth, ranged between 0.18 (Q38_mGr, 100–250 µm) and 1.0 (Q2_cSa, 250–500 µm) (Table 3, Fig. 4). Low values of λ_L represent a low filtering effect of the sediment, i.e. MPPs are substantially relocated to greater depth, whereas high values of λ_L correspond to a high filtering effect of the sediment, i.e. MPPs are retained already in the first centimetres of the sediment (Fig. 4).

The filter coefficient was found to

- continuously increase with increasing MPP size,
- continuously decrease with increasing flow rate, and
- substantially decrease with increasing sediment particle size.

These general relations did apply with exception for the comparison between Q2_cSa and Q4_cSa. Here the filter coefficient for the flow rate of 4 ml min^{-1} is slightly larger than for 2 ml min^{-1}, not smaller. It may be Q4_cSa that deviates from the general relations of the filter coefficients due to slight unknown differences in the column sediment structure affecting the particle transport (experimental error). For Q4_cSa the particle abundance at 5–10 cm and 15–20 cm is slightly higher than the particle abundance in 2.5–5 cm depths (Fig. S5 in Supporting Information). This peculiarity also affects the value and the quality of the estimated filter coefficient for this column. The goodness of fit between theoretical and experimental retention profile for Q4_cSA, size class 100–250 µm ($R^2 = 0.40$) was substantially lower than for all our remaining experiments (average R^2 for all model fits = 0.86, Tab. S6 in Supporting Information). The good model fits furthermore verify that MPP abundance decreases exponentially with increasing depth, as is typical for a particle filtration.

The average difference in filter coefficient between the size class of 100–250 µm and 250–500 µm of all gravel filled and sand filled columns was 0.05 cm^{-1} and 0.24 cm^{-1}, respectively (Table 3). The filter coefficient of all gravel packed columns increased on average by 0.015 per decrease of 1 m d^{-1} (1.4 ml min^{-1}) in flow velocity. These results extend studies previously limited to very small, primary PS spheres (< 10 µm) [3, 4, 9] to more realistic circumstances and show that particle transport of PS fragments strongly depend on the hydrodynamics, and the colloid and collector grain sizes.

Table 3 Overview of optimized filter coefficient values of each column and particle size class, as far as applicable. The corresponding R^2 and standard error is listed in Tab. S6 in the Supporting Information

Column name	Filter coefficient (λ_L) [cm^{-1}]		
	100–250 µm	250–500 µm	500–1000 µm
Q38_mGr	0.18	0.26	0.32
Q20_mGr	0.28	0.29	0.33
Q13_mGr	0.38	0.38	0.53
Q4_mGr	0.48	0.59	
Q10_mGr_4PV	0.42	0.43	0.56
Q10_mGr_2PV	0.38	0.43	0.83
Q4_cSa*[1]	0.83	1.03	
Q2_cSa	0.71	0.99	
Q6_cSa_2PV	0.67		
Q11_cSa_4PV	0.50	0.77	

* may have been influenced by experimental errors (e.g. heterogeneous sediment layers)

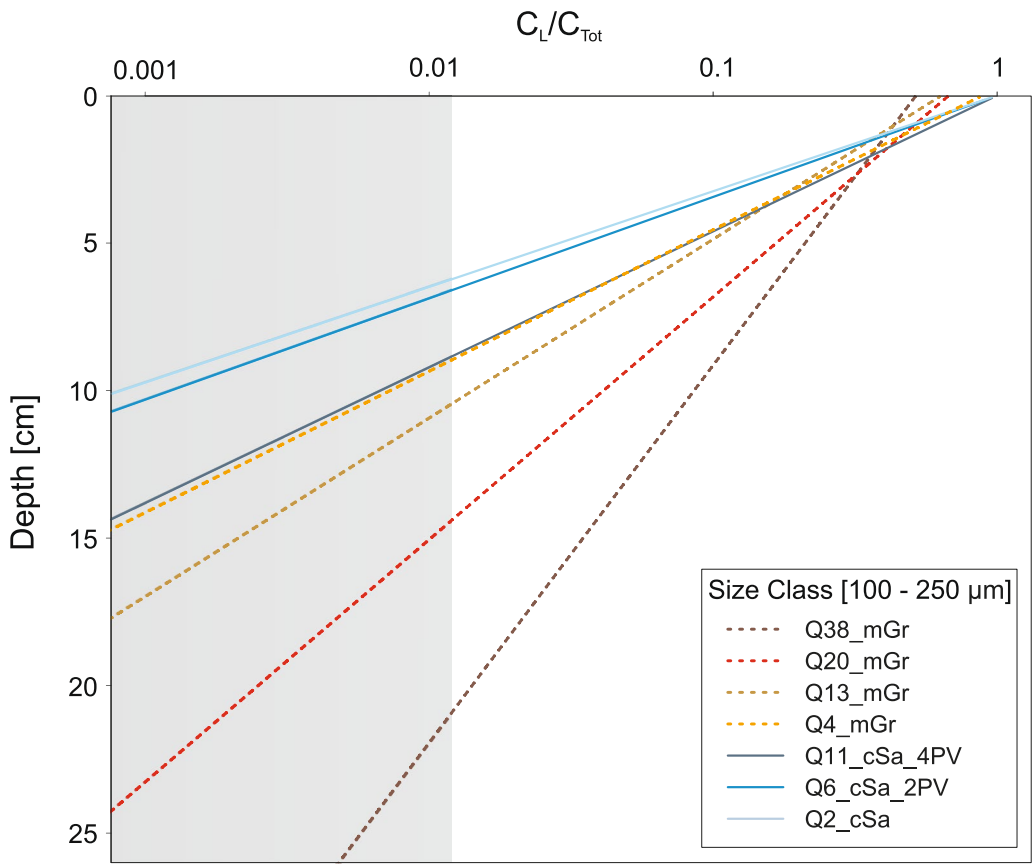

Fig. 4 Comparison of PS retention profiles of the particle Size Class from 100 to 250 µm. Note that y-axis is log scaled. Below a particle abundance of 0.023 (area highlighted in light grey), the observed change in particle abundance with increasing depth partly deviates from the exponential model assumption

We also examined more systematically how the MPP retention (quantified by the filter coefficient) is related to dimensionless flow velocity, MPP and sediment grain sizes. GLM regression was performed using the log transformation as link function. Fig. 5 depicts the effect of the seepage velocity for different MPP size and sediment particle size on $\log(\lambda_L)$ [λ_L in cm^{-1}] . The applied GLM revealed significant effects of all predictors on the filter coefficient (p-value < 0.01, $R^2 = 0.92$):

$$\lambda_L{}^* = \log(\lambda_L) = -0.24 + 0.44 \times \frac{minFeret_L}{minFeret_{L,mean}} - 0.32 \times \frac{v_a}{v_{a,mean}} - 0.47 \times \frac{d_{50}}{d_{50,mean}} \quad (4)$$

Because the estimated beta values hardly differ, it can be concluded that the influence of each predictor on the filter coefficient is comparable magnitude (d_{50} has a slightly greater influence on the retention behavior of MPPs than v_a). The $minFeret_L$ is specific for a certain MPP size class (L) and therefore linearly influences the offset of the multiple GLM but with an overall significant effect on the filter coefficient. Just considering a GLM with a single predictor revealed a significant effect of v_a ($R^2 = 0.64$) and d_{50} ($R^2 = 0.47$) on $\lambda_L{}^*$ (details of the GLM's are shown in Table S7 & S8 in the Supporting Information).

Equation 4 allows to estimate retention of microplastic fragments in riverbed sediments and alluvial aquifers mainly consisting of medium sands and large gravels. In other words, by an approximate estimate of the filter coefficient (eq. 4), the retention profiles of MPPs in rough porous media (eq. 2) and the maximum depth of particle appearance in riverbeds can be calculated based on the prevailing environmental conditions (flow velocity, MPP and median sediment particle size).

In summary, while experimental sediment columns provide a mechanistic insight into microplastic transport, their findings should be interpreted with caution

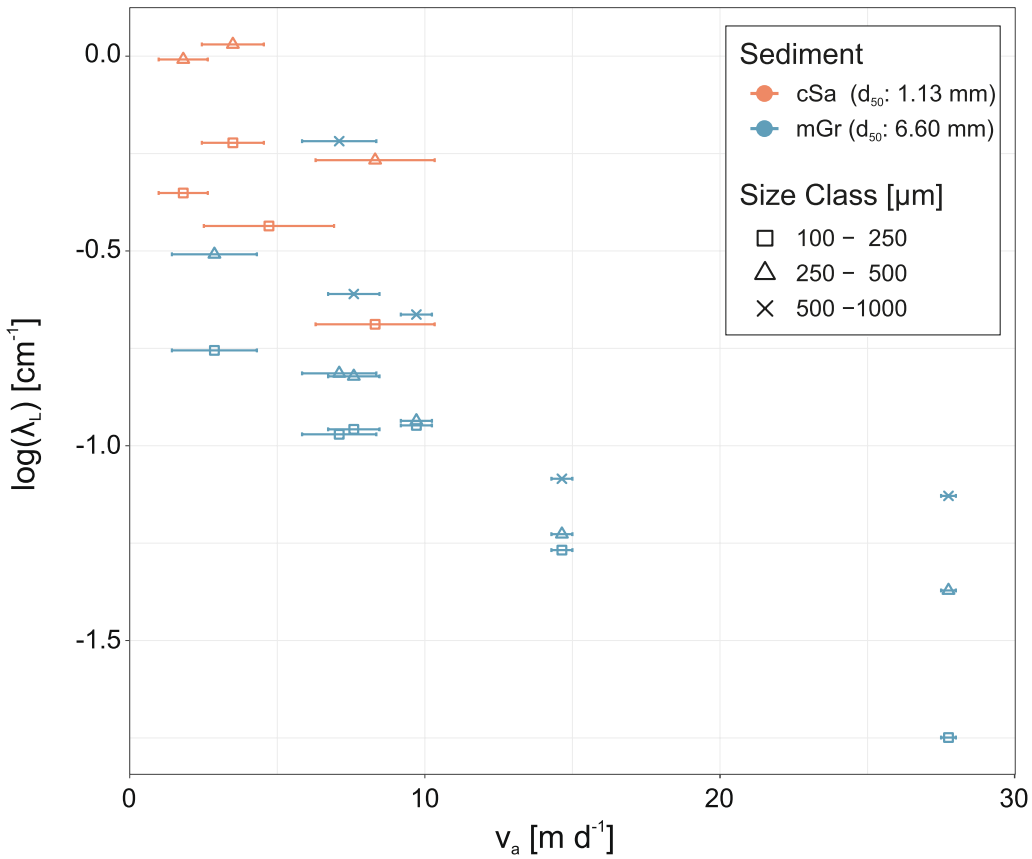

Fig. 5 Relation between flow rate and filter coefficient (λ_L). The bars depict the standard deviation of the averaged flow velocities. Due to better readability, the generally quite small standard error of λ_L was not displayed. These values are listed in Table S6 in the supporting information

when extrapolating to natural riverine systems due to the inherent complexities and dynamics.

- Natural riverbeds often exhibit a wide range of sediment types, including various particle sizes and organic content that are not accounted for in the current experiments.
- River flow is dynamic and influenced by various factors such as channel morphology, flow velocity, and turbulences. In laboratory settings, flow conditions are typically simplified, e.g. no lateral forces on top of the infiltration point were present that can cause horizontal particle movement or particle remobilization)
- Natural riverbeds are teeming with diverse microbial and macroinvertebrate communities. Their activities, such as bioturbation and biofilm formation, can significantly alter microplastic transport patterns.
- River systems experience seasonal fluctuations in flow rates, sedimentation patterns, and MPP loads.

These aspects can explain heterogeneous retention profiles of MPPs found in natural riverbed sediments [14] and the occurrence of large particles in relatively high streambed depth [15] that could not be explained by MPP transport with infiltrating surface water alone. So far eq. 4 is only valid for PS fragments in the applied range of seepage velocity, MPP size, and sediment particle size. In the experiments only organic free, homogeneous sediment materials with a narrow grain size distributions were considered. Extrapolations beyond that range should be treated with caution.

Nevertheless, this study provides a mechanistic approach to estimate retention profiles and advective transport distance of MPPs in riverbed sediments caused by surface water infiltration. Our results show that river sediments represent both, a potential sink of MPP due to the high retention within the first cm of sediment but also a potential pathway of pore scale microplastics (100–500 µm) from surface waters to hyporheic zones and aquifers. The much larger proportion of MPPs are, at least temporarily, immobilized in the streambeds. Overall, this expands our ability to understand transport behaviour and distribution of MPP in river and lake bottom sediments.

Conclusions

Plastic pollution is a global and pervasive problem in freshwater ecosystems. The results of these column studies highlight that MPPs are generally retained in saturated sediments, although in dependence of flow velocity, sediment grain and MPP size. In the gravel packed columns all particles above 1000 µm were retained on the uppermost 5 cm. MPPs in between 500 and 1000 µm could infiltrate to an average depth of 20 cm whereas MPP below 500 µm in size were relocated to depth of 50 cm for high flow velocities. In the sand packed columns MPPs above 500 µm were retained in the uppermost 2.5 cm whereas MPPs below 500 µm infiltrated to an average depth of 15 cm. Nevertheless, some MPPs below 500 µm were transported down the full length of the column and thus could pass larger distances than that. This implies that MPP < 500 µm on the pore scale can indeed be advectively transferred into coarse grained sediments, can remain mobile and thus pose a potential threat to ground- and drinking water analogous to dissolved substances in induced bank filtration [26].

In general, it seems that already within 2 PV of water flow the major part of MPP retention has been occurring and afterwards no substantial relocation of MPP occurs, at least if conditions remain stable and no further MPP input happens. We observed an exponential decrease in MPP abundance with increasing depth, which significantly depends on flow velocity, sediment grain and MPP size and can be well described by first-order deep filtration theory. We therefore assume that MPP distributions in natural riverbed sediments, which deviate from this theoretical behavior, are influenced by a variety of dynamic processes such as variable sedimentation rates, remobilization, and sediment rearrangements. However, there is still an urgent need to further mechanistically unravel the role of environmental factors affecting the transport.

Supplementary Information

The online version contains supplementary material available at https://doi.org/10.1186/s43591-023-00077-z.

Additional file 1.

Acknowledgements

Special thanks to the technical staff of the Federal Waterways Engineering and Research Institute (BAW), namely Mr. Rafael Roost, for helpful discussions and construction of the columns and the sediment extraction pushing device. We acknowledge the Fraunhofer-ICT and Dr. Mathias Bochow to provide grinded polystyrene particles. We thank Anja Schlör and Dr. Martin Listek from the Department of Immunotechnology at the University of Potsdam, who introduced us to the use of to the fluorescence imaging system ChemiDoc and provided access to it.

Authors' contributions

All authors conceived the study; M.P. designed the columns and sediment extraction pushing device; C.L and D.P. conducted the experiments and analysed the data; C.L. created the ImageJ macro; M.M. conducted the statistical analyses and led the writing of the manuscript; S.O., M.M. and M.P. supervised the study; all authors contributed to writing of the manuscript.

Funding

Open Access funding enabled and organized by Projekt DEAL. This work was supported by the Federal Waterways Engineering and Research Institute (BAW) in Karlsruhe, Germany. Funded by the Deutsche Forschungsgemeinschaft (DFG, German Research Foundation) – project number 491466077.

Availability of data and materials

The datasets used and analyzed during the current study are publicly available on Zenodo (https://doi.org/10.5281/zenodo.8055599).

Declarations

Ethics approval and consent to participate

Not applicable.

Consent for publication

Not applicable.

Competing interests

The authors declare no competing interests.

Received: 12 June 2023 Accepted: 27 November 2023
Published online: 15 January 2024

References

1. Alimi OS, Farner Budarz J, Hernandez LM, Tufenkji N. Microplastics and Nanoplastics in aquatic environments: aggregation, deposition, and enhanced contaminant transport. Environ Sci Technol. 2018;52:1704–24. https://doi.org/10.1021/acs.est.7b05559.
2. Boos J-P, Gilfedder BS, Frei S. Tracking microplastics across the streambed Interface: using laser-induced-fluorescence to quantitatively analyze microplastic transport in an experimental flume. Water Resour Res. 2021;57:e2021WR031064. https://doi.org/10.1029/2021WR031064.
3. Bradford SA, Torkzaban S, Walker SL. Coupling of physical and chemical mechanisms of colloid straining in saturated porous media. Water Res. 2007;41:3012–24. https://doi.org/10.1016/j.watres.2007.03.030.
4. Bradford SA, Yates SR, Bettahar M, Simunek J. Physical factors affecting THE transport and fate of colloids in saturated porous media: FACTORS AFFECTING THE FATE OF COLLOIDS. Water Resour Res. 2002;38:63-1–63–12. https://doi.org/10.1029/2002WR001340.
5. Buades A, Coll B, Morel J-M. Non-local means Denoising. Image Process On Line. 2011;1:208–12.
6. Chambers JM, Hastie T. Statistical models in S, Wadsworth & BrooksCole computer science series. Wadsworth & BrooksCole Advanced Books & Software; 1992.
7. Corcoran PL, Belontz SL, Ryan K, Walzak MJ. Factors controlling the distribution of microplastic particles in Benthic sediment of the Thames River, Canada. Environ Sci Technol. 2020;54:818–25. https://doi.org/10.1021/acs.est.9b04896.
8. Dong S, Cai W, Xia J, Sheng L, Wang W, Liu H. Aggregation kinetics of fragmental PET nanoplastics in aqueous environment: complex roles of electrolytes, pH and humic acid. Environ Pollut. 2021;268:115828. https://doi.org/10.1016/j.envpol.2020.115828.
9. Dong Z, Qiu Y, Zhang W, Yang Z, Wei L. Size-dependent transport and retention of micron-sized plastic spheres in natural sand saturated with seawater. Water Res. 2018;143:518–26. https://doi.org/10.1016/j.watres.2018.07.007.
10. Dris R, Imhof H, Sanchez W, Gasperi J, Galgani F, Tassin B, et al. Beyond the ocean: contamination of freshwater ecosystems with (micro-) plastic particles. Environ Chem. 2015;12:539. https://doi.org/10.1071/EN14172.
11. Drummond JD, Nel HA, Packman AI, Krause S. Significance of Hyporheic exchange for predicting microplastic fate in Rivers. Environ Sci Technol Lett. 2020;7:727–32. https://doi.org/10.1021/acs.estlett.0c00595.
12. Elagami H, Ahmadi P, Fleckenstein JH, Frei S, Obst M, Agarwal S, et al. Measurement of microplastic settling velocities and implications

for residence times in thermally stratified lakes. Limnol Oceanogr. 2022;67:934–45. https://doi.org/10.1002/lno.12046.
13. Fox J, Monette G. R and S-plus companion to applied regression. USA: Sage Publications, Inc.; 2002.
14. Fraser MA, Chen L, Ashar M, Huang W, Zeng J, Zhang C, et al. Occurrence and distribution of microplastics and polychlorinated biphenyls in sediments from the Qiantang River and Hangzhou Bay. China Ecotoxicol Environ Saf. 2020;196:110536. https://doi.org/10.1016/j.ecoenv.2020.110536.
15. Frei S, Piehl S, Gilfedder BS, Löder MGJ, Krutzke J, Wilhelm L, et al. Occurence of microplastics in the hyporheic zone of rivers. Sci Rep. 2019;9:15256. https://doi.org/10.1038/s41598-019-51741-5.
16. Iwasaki T, Slade JJ, Stanley WE. Some notes on sand filtration [with discussion]. J (Am Water Works Assoc). 1937;29:1591–602.
17. Koelmans AA, Mohamed Nor NH, Hermsen E, Kooi M, Mintenig SM, De France J. Microplastics in freshwaters and drinking water: critical review and assessment of data quality. Water Res. 2019;155:410–22. https://doi.org/10.1016/j.watres.2019.02.054.
18. Kumar R, Sharma P, Manna C, Jain M. Abundance, interaction, ingestion, ecological concerns, and mitigation policies of microplastic pollution in riverine ecosystem: a review. Sci Total Environ. 2021a;782:146695. https://doi.org/10.1016/j.scitotenv.2021.146695.
19. Kumar R, Sharma P, Verma A, Jha PK, Singh P, Gupta PK, et al. Effect of physical characteristics and hydrodynamic conditions on transport and deposition of microplastics in riverine ecosystem. Water. 2021b;13:2710. https://doi.org/10.3390/w13192710.
20. Li J, Liu H, Paul Chen J. Microplastics in freshwater systems: a review on occurrence, environmental effects, and methods for microplastics detection. Water Res. 2018a;137:362–74. https://doi.org/10.1016/j.watres.2017.12.056.
21. Li S, Liu H, Gao R, Abdurahman A, Dai J, Zeng F. Aggregation kinetics of microplastics in aquatic environment: complex roles of electrolytes, pH, and natural organic matter. Environ Pollut. 2018b;237:126–32. https://doi.org/10.1016/j.envpol.2018.02.042.
22. Lim SJ, Seo J, Hwang M, Kim H-C, Kim E-J, Lee J, et al. A multiscale framework for modeling transport of microplastics during sand filtration: bridging from pore to continuum. J Hazard Mater. 2023;443:130219. https://doi.org/10.1016/j.jhazmat.2022.130219.
23. Maes T, Jessop R, Wellner N, Haupt K, Mayes AG. A rapid-screening approach to detect and quantify microplastics based on fluorescent tagging with Nile red. Sci Rep. 2017;7:44501. https://doi.org/10.1038/srep44501.
24. Mintenig SM, Löder MGJ, Primpke S, Gerdts G. Low numbers of microplastics detected in drinking water from ground water sources. Sci Total Environ. 2019;648:631–5. https://doi.org/10.1016/j.scitotenv.2018.08.178.
25. Munz M, Kreiß J, Krüger L, Schmidt LK, Bochow M, Bednarz M, et al. Application of high-resolution near-infrared imaging spectroscopy to detect microplastic particles in different environmental compartments. Water Air Soil Pollut. 2023;234:286. https://doi.org/10.1007/s11270-023-06245-4.
26. Munz M, Oswald SE, Schäfferling R, Lensing H-J. Temperature-dependent redox zonation, nitrate removal and attenuation of organic micropollutants during bank filtration. Water Res. 2019;162:225–35. https://doi.org/10.1016/j.watres.2019.06.041.
27. Munz M, Oswald SE, Schmidt C. Coupled long-term simulation of reach-scale water and heat fluxes across the river-groundwater Interface for retrieving Hyporheic residence times and temperature dynamics. Water Resour Res. 2017;53:8900–24. https://doi.org/10.1002/2017WR020667.
28. Niu L, Li Y, Li Y, Hu Q, Wang C, Hu J, et al. New insights into the vertical distribution and microbial degradation of microplastics in urban river sediments. Water Res. 2021;188:116449. https://doi.org/10.1016/j.watres.2020.116449.
29. Nizzetto L, Bussi G, Futter MN, Butterfield D, Whitehead PG. A theoretical assessment of microplastic transport in river catchments and their retention by soils and river sediments. Environ Sci Process Impacts. 2016;18:1050–9. https://doi.org/10.1039/c6em00206d.
30. Pittroff M, Müller YK, Witzig CS, Scheurer M, Storck FR, Zumbülte N. Microplastic analysis in drinking water based on fractionated filtration sampling and Raman microspectroscopy. Environ Sci Pollut Res. 2021;28:59439–51. https://doi.org/10.1007/s11356-021-12467-y.
31. Pivokonsky M, Cermakova L, Novotna K, Peer P, Cajthaml T, Janda V. Occurrence of microplastics in raw and treated drinking water. Sci Total Environ. 2018;643:1644–51. https://doi.org/10.1016/j.scitotenv.2018.08.102.
32. Prata JC, da Costa JP, Lopes I, Duarte AC, Rocha-Santos T. Environmental exposure to microplastics: an overview on possible human health effects. Sci Total Environ. 2020;702:134455. https://doi.org/10.1016/j.scitotenv.2019.134455.
33. Prata JC, Reis V, Matos JTV, da Costa JP, Duarte AC, Rocha-Santos T. A new approach for routine quantification of microplastics using Nile red and automated software (MP-VAT). Sci Total Environ. 2019;690:1277–83. https://doi.org/10.1016/j.scitotenv.2019.07.060.
34. R Core Team. R: a language and environment for statistical computing. Vienna, Austria: R Foundation for Statistical Computing; 2021.
35. Rahman A, Sarkar A, Yadav OP, Achari G, Slobodnik J. Potential human health risks due to environmental exposure to nano- and microplastics and knowledge gaps: a scoping review. Sci Total Environ. 2021;757:143872. https://doi.org/10.1016/j.scitotenv.2020.143872.
36. Ren Z, Gui X, Xu X, Zhao L, Qiu H, Cao X. Microplastics in the soil-groundwater environment: aging, migration, and co-transport of contaminants – a critical review. J Hazard Mater. 2021;419:126455. https://doi.org/10.1016/j.jhazmat.2021.126455.
37. Rummel CD, Jahnke A, Gorokhova E, Kühnel D, Schmitt-Jansen M. Impacts of biofilm formation on the fate and potential effects of microplastic in the aquatic environment. Environ Sci Technol Lett. 2017;4:258–67. https://doi.org/10.1021/acs.estlett.7b00164.
38. Sarijan S, Azman S, Said MIM, Jamal MH. Microplastics in freshwater ecosystems: a recent review of occurrence, analysis, potential impacts, and research needs. Environ Sci Pollut Res. 2021;28:1341–56. https://doi.org/10.1007/s11356-020-11171-7.
39. Schmidt LK, Bochow M, Imhof HK, Oswald SE. Multi-temporal surveys for microplastic particles enabled by a novel and fast application of SWIR imaging spectroscopy – study of an urban watercourse traversing the city of Berlin, Germany. Environ Pollut. 2018;239:579–89. https://doi.org/10.1016/j.envpol.2018.03.097.
40. Schneider CA, Rasband WS, Eliceiri KW. NIH image to ImageJ: 25 years of image analysis. Nat Methods. 2012;9:671–5. https://doi.org/10.1038/nmeth.2089.
41. Tötzke C, Kozhuharova B, Kardjilov N, Lenoir N, Manke I, Oswald SE. Non-invasive 3D analysis of microplastic particles in sandy soil - Exploring feasible options and capabilities. Sci Total Environ. 2024;907:167927. https://doi.org/10.1016/j.scitotenv.2023.16792.
42. Tötzke C, Oswald SE, Hilger A, Kardjilov N. Non-invasive detection and localization of microplastic particles in a sandy sediment by complementary neutron and X-ray tomography. J Soils Sediments. 2021;21:1476–87. https://doi.org/10.1007/s11368-021-02882-6.
43. Tumwet FC, Serbe R, Kleint T, Scheytt T. Effect of fragmentation on the transport of polyvinyl chloride and low-density polyethylene in saturated quartz sand. Sci Total Environ. 2022;836:155657. https://doi.org/10.1016/j.scitotenv.2022.155657.
44. Waldschläger K, Brückner M, Almroth B, Hackney C, Adyel T, Alimi O, et al. Learning from natural sediments to tackle microplastics challenges: a multidisciplinary perspective. Earth Sci Rev. 2022;228:104021. https://doi.org/10.1016/j.earscirev.2022.104021.
45. Waldschläger K, Schüttrumpf H. Infiltration behavior of microplastic particles with different densities, sizes, and shapes—from glass spheres to natural sediments. Environ Sci Technol. 2020;54:9366–73. https://doi.org/10.1021/acs.est.0c01722.
46. Waldschläger K, Schüttrumpf H. Effects of particle properties on the settling and rise velocities of microplastics in freshwater under laboratory conditions. Environ Sci Technol. 2019;53:1958–66. https://doi.org/10.1021/acs.est.8b06794.
47. Wett B, Jarosch H, Ingerle K. Flood induced infiltration affecting a bank filtrate well at the river Enns, Austria. J Hydrol. 2002;266:222–34. https://doi.org/10.1016/S0022-1694(02)00167-1.
48. Wondzell SM. Effect of morphology and discharge on hyporheic exchange flows in two small streams in the Cascade Mountains of Oregon. USA Hydrol Process. 2006;20:267–87. https://doi.org/10.1002/hyp.5902.

Publisher's Note